A Fast Open-Switch Fault and Open-Winding Fault Distinguish Method Based on Voltage Reference Modification

Xinxiu Zhou, *Member, IEEE*, Qingyao Hu, Peiling Cui, *Member, IEEE*, Xueping Xu, and Kun Mao

***Abstract*—Similar postfault current behaviors make it difficult to distinguish open-winding fault and open-switch fault quickly and accurately, which may lead to motor performance degrade seriously. Although several methods were proposed to distinguish them, they take too long time and false detection often occurs. To solve this issue, a reference voltage correction-based fault distinguish method is proposed in this article. First, an improved adaptive residuals threshold is designed based on the quantitative analysis of residual. It is simple and insensitive to motor operation condition. As a result, the fault can be detected accurately. Second, the relationship between residuals and reference current in open-switch fault and open-winding fault is analyzed, respectively. Based on this relationship, reference voltage correction-based fault location method is proposed. Through varying the reference voltage polarity, the reference current polarity and residual vectors polarity can be changed accordingly. Then, according to the polarity of residual vectors, the fault can be distinguished and located in a shorter time. Finally, the rapidity and accuracy of the fault distinguish method is verified by experimental results.**

***Index Terms*—Fault distinguish, fault location, open-switch fault, open-winding fault, permanent magnet motor.**

I. Introduction

PERMANENT magnet synchronous motor (PMSM) has been applied in various applications owing to its high-power density and high efficiency [1], [2], [3]. However, unpredictable faults may occur in motor winding and driver. As a result, the PMSM performance would degrade and damage may occur.

Motor electrical fault can be divided into winding failure and driver failure which account for 37% [4], [5], [6] and 38% [7], respectively. These two kinds of fault are mainly caused by open-circuit fault and short-circuit fault. Short-circuit fault is destructive, and the induced overheating and overcurrent may damage the motor. Various methods have been proposed to diagnose short-winding fault and it can be detected at early stage. While short-switch fault is always detected by hardware and converted to open-switch fault [8], [9]. As for the open-winding fault and open-switch fault, both of them may lead to motor phase current distortion, torque fluctuation, and control performance degrade. In addition, secondary failures would be induced if the motor continuously drives. Hence, accurate open-circuit fault detection and fast fault localization is not a trivial task but worth studying.

Open-switch/winding faults in different constructure PMSM have been widely studied, such as three-phase motor, five-phase motor [10], dual three-phase motor [11], [12], [13], [14], and the motor with more phases [15]. However, most of methods proposed in the previous literature are based on the analysis of each phase. Normally, they can be extended to other kinds of motor in principle. Compared with multiphase motor, three-phase motors are widely used in industry applications. Hence, it is significant to study fault diagnosis method for three-phase PMSM.

Generally, the fault detection methods can be classified as model-free methods and model-based methods. Model-free methods are easy to be implemented. It can be further divided into voltage-based methods [17], [18] and current-based methods [19], [20], [21], [22]. The former methods possess faster diagnostic speed. But it requires extra measurement circuit which increases the system cost and complexity. Besides, this kind of method is susceptible to interferences. In the latter methods, fault is detected by extracting fault sensitive index from motor current. In this method, extra hardware can be avoided, but it is sensitive to load variation and longer diagnostic time is required. Through current index's normalization, load dependence can be avoided. But its diagnostic time is still too long [20], [21]. As for the model-based method, its fault diagnosis speed is faster. Through monitoring the residual, i.e., the difference between the estimated variables with actual variables in real-time, the fault can be detected [23], [24], [25], [26], [27], [28], [29], [30], [31], [32]. In this method, observers are employed for estimating the motor state variables. As the observer may be influenced by motor operation condition and parameter uncertainties, misdiagnosis often occurs. To overcome this problem, differential current observer is proposed [31]. In this observer, motor parameter estimation error is taken into account. Therefore, better robustness can be obtained. In [32], parameter uncertainty and load change are observed through the disturbance observer. Hence, its sensitivity to parameters and load can be reduced. The above model-based

Manuscript received 16 October 2022; revised 14 February 2023 and 12 April 2023; accepted 16 May 2023. Date of publication 31 May 2023; date of current version 28 July 2023. This work was supported by the National Natural Science Foundation of China under Grants 62122009 and 62073021. Recommended for publication by Associate Editor J. Hur. *(Corresponding author: Peiling Cui)*

The authors are with the School of Instrumentation Science and Opto -Electronics Engineering, Beihang University, Beijing 100191, China (e-mail: 580927@163.com; huqingyao@buaa.edu.cn; cuiplhh@126.com; xuxueping@buaa.edu.cn; kunmao@buaa.edu.cn).

Color versions of one or more figures in this article are available at https://doi.org/10.1109/TPEL.2023.3281683.

Digital Object Identifier 10.1109/TPEL.2023.3281683

fault detection approaches [31], [32] have advantages such as faster diagnosis speed and parameter error robust. However, there are still some problems as follows.

1) Unsuitable thresholds would lead to false detection directly. However, adaptive thresholds design is rarely involved in previous diagnosis methods.
2) Postfault current behaviors of open-winding fault and open-switch fault are similar. However, conventional fault detection methods cannot distinguish them.

Therefore, the previous techniques are not suitable for fault distinguishment, and little research has been done on the adaptive thresholds design. Further studies are still necessary.

Through comparing the residuals and thresholds, the fault can be judged. It is found that the residual magnitude varies with motor operation states [4] and it may deviate from zero without fault [33]. Note that if fixed threshold is set, the lower thresholds may lead to false detection under heavy load, while the higher value would cause missed detection. Its value needs to be regulated according to the motor operation point and parameters perturbation [29]. Fixed threshold is not suitable for the variable operation conditions. It is necessary to design a decent adaptive threshold for the satisfactory motor operations.

It is expected that the threshold is greater than residual prefault, while lower than its postfault. In order to achieve this goal, *d–q* current is observed to construct current residual index current form factors (CFF), and normalized current is utilized to reduce the sensitivity to load variation in paper [27]. CFF obtained by observer is used as threshold to compare with that calculated by actual currents. Although this index is insensitive to motor operation condition, the difference between actual and observed CFF is compared with a fixed threshold which leads to inferior robustness. After that, a variable relates to motor dynamic performance and its operating point is introduced into the threshold algorithm [29]. This method shows better robustness against load variation. However, the selection of threshold depends on the gain of observer, which needs to be constantly adjusted. Besides, the threshold amplitude tends to increase after fault. It may lead to miss diagnosis when comparing with increasing residuals. Moreover, its effectiveness has not been verified under variable speed and its robustness against parameter variation is unknown. In [30], sampling error, parameters error, dead time, etc., are included in the threshold to consider practical applications. This method can detect faut under speed change and load change. In [31], adaptive threshold is designed based on the residual state equation obtained by differential current observer. It changes with the motor operating conditions which make it robust to speed and load variation. Besides, parameter errors are taken into account. Hence, this method can avoid the influence of parameter variations. However, this threshold design method is very complicate and parameters dependent.

Through the above methods, it can be found that the threshold can be designed robust to operation conditions and parameter changes. But they are more complex and difficult to be applied in practice.

Once the fault is detected, accurate fault localization is immediately required. However, similar postfault current performance of the open-switch fault and open-winding fault makes it difficult to locate the fault. If fault location is wrong, serious damage would be induced. Hence, it is necessary to distinguish and locate open-switch fault and open-winding fault in time. Although open-switch fault and open-winding fault can be distinguished by some methods, they are complicated and sensitive. As a result, misdiagnosis and missed diagnosis often occur.

In [34], the determination of the open-winding fault and open-switch fault needs several comparisons of different indicators and thresholds. The thresholds are difficult to be determined. Besides, false alarms may generate during open-winding fault diagnosis. In [21], average normalized current value was used to distinguish open-switch fault and open-winding fault. But it is time-consuming. Similarly, a method based on average absolute currents was proposed to identify the fault type in [34] and [36]. It costs almost one electric cycle. In [37], the zero-sequence voltage fundamental component and the initial stator currents phase differences were combined to realize the discrimination of open-phase fault. Its diagnosis time reduces by 44%. But it is still too long compared with the time just to detect the fault. In [38], the faulty phase was located by comparing the current deviations in *dq*-axis. And then, the faults can be located within three specific faults (upper/lower switch fault or open-winding fault on the same phase). Specific fault can be detected within several switching periods. However, its fixed threshold and active intervention time have great influence on diagnosis accuracy. Besides, the performance of the method heavily depends on motor parameters. Therefore, it is difficult to be applied in different kind of motors.

Through the above analyses it can be found that the existing methods are complicated and time-consuming. Besides, their applicability is also limited.

According to the previous studies, there are two main issues in open-switch fault and open-winding fault diagnosis. First, it is difficult to design a threshold which is simple and robust to the changes of motor operation conditions. Second, it is time-consuming to distinguish faults and it is difficult to be applied in different kinds of motors. To solve the above problems, a new adaptive threshold is designed based on the law of current residual. As a result, superior robustness can be obtained. Furthermore, it is simple and easy to be realized. To accelerate distinguished speed, a reference voltage correction-based location method is designed. By changing the polarity of the voltage, the polarity of the current and the residuals can be changed accordingly. Based on the variation of the residuals, fault can be distinguished and located in a short time. It can be easily applied in different motors with different parameters compared with previous methods.

II. Fault Features of Open-Switch Fault and Open-Winding Fault

A. Features of Open-Winding Fault

The topological diagram of PMSM three-phase inverter is described in Fig. 1.

Assuming that the PMSM three-phase windings are symmetrical, the three-phase voltage equation can be written as follows:

$$\boldsymbol{u}_{abc} = \boldsymbol{R} \cdot \boldsymbol{i}_{abc} + \boldsymbol{L}_s \cdot \mathrm{p} \cdot \boldsymbol{i}_{abc} + \boldsymbol{e}_{abc} \tag{1}$$

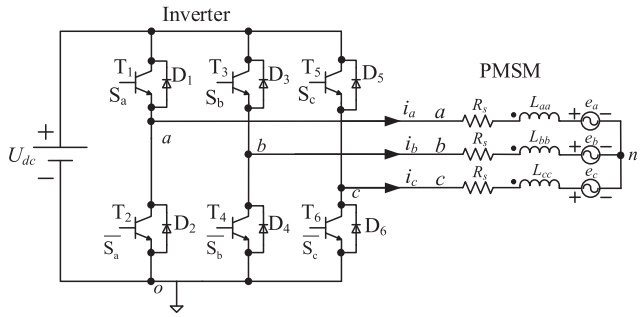

Fig. 1. PMSM three-phase inverter topological diagram.

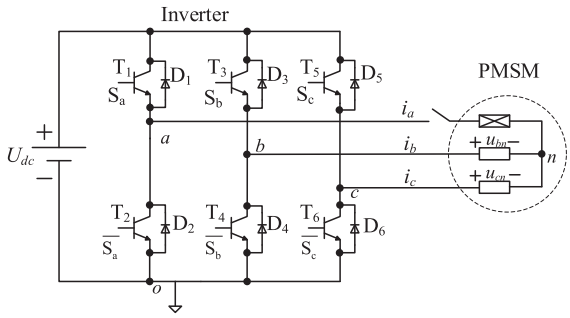

Fig. 2. Winding an open fault topological diagram.

where $\boldsymbol{u_{abc}} = [u_{an}\ u_{bn}\ u_{cn}]^{\mathrm{T}}$, u_{an}, u_{bn}, and u_{cn} are the three-phase voltages, $\boldsymbol{i_{abc}} = [i_a\ i_b\ i_c]^{\mathrm{T}}$, i_a, i_b, and i_c are motor phase currents, p is the differential operator, R is the resistance matrix, $\boldsymbol{R}$= [r 00; 0 r 0; 00 r], and L_s is the inductance matrix, $L_s = [LMM; MLM; MML]$, $e_{abc} = [e_a e_b e_c]^T$ is three-phase back electromotive forces, respectively.

The relationship between motor terminal voltages and phase voltages can be generally expressed as follows [25]:

$$u_{xn}=(2u_{xo} - u_{yo} - u_{zo})/3 \tag{2}$$

where subscripts $x, y, z \in \{a, b, c\}$, u_{xo}, u_{yo}, u_{zo} are the three-phase terminal voltages with respect to ground, respectively.

In order to analyze fault features, the open-fault in winding A is taken as an example here, as shown in Fig. 2. When winding A opens, the current in phase A drops to 0 rapidly. In the meantime, distortions present in the other two phases can be utilized to diagnose the fault. Hence, the change laws of motor voltages under faulty conditions are analyzed.

Considering that motor inductance value is small, it can be neglected in (1). When winding A opens, its current drops to 0. Substituting $i_a = 0$ into (1), the phase voltage can be rewritten as follows:

$$u_{an} \approx e_a. \tag{3}$$

Substituting (3) into (2), the terminal voltage u_{ao} can be derived as follows:

$$u_{ao}=\frac{1}{2}\cdot(3e_a + u_{bo} + u_{co}),\ i_a = 0. \tag{4}$$

TABLE I
RELATIONSHIPS AMONG PMSM KEY VARIABLES DURING WINDING FAULTS

Faulty winding	Voltage distortions	Current reference polarity	Phase current
Winding A	$\Delta u_{ao} < 0$	$i_a^* > 0$	$i_a = 0$
	$\Delta u_{ao} > 0$	$i_a^* < 0$	
Winding B	$\Delta u_{bo} < 0$	$i_b^* > 0$	$i_b = 0$
	$\Delta u_{bo} > 0$	$i_b^* < 0$	
Winding C	$\Delta u_{co} < 0$	$i_c^* > 0$	$i_c = 0$
	$\Delta u_{co} > 0$	$i_c^* < 0$	

Then, through comparing the measured value with the reference value, the voltage distortion can be calculated

$$\begin{aligned}\Delta u_{ao} &= u_{ao} - u_{ao}^* = \frac{1}{2}\cdot(3e_a + u_{bo}^* + u_{co}^*) - u_{ao}^* \\ &= -\frac{3}{2}\cdot(u_{an}^* - e_a)\end{aligned} \tag{5}$$

where Δu_{ao} is the terminal voltage distortion of the phase A, and $u_{ao}{}^*$ and $u_{an}{}^*$ are the terminal voltage command and phase voltage reference of phase A, respectively.

According to (1)

$$u_{an} - e_a = R_s i_a + (L - M)\frac{di_a}{dt} \approx Z_L i_a \tag{6}$$

where Z_L is the impedance of the stator winding, it can be expressed as $Z_L = \sqrt{R_s^2 + \omega_e^2(L-M)^2}$.

The analyses of other windings open faults are similar.

Generally, the terminal voltage distortions of open-winding fault can be expressed as follows:

$$\Delta u_{xo} = u_{xo} - u_{xo}^* \approx -\frac{3}{2}\cdot Z_L i_x^* \tag{7}$$

where Δu_{xo} is the terminal voltage distortion of the phase x (subscripts $x \in \{a, b, c\}$), $u_{xn}{}^*$ is the voltage reference, and $i_x{}^*$ is the current reference, respectively.

It can be noticed that Δu_{xo} is negative proportional to $i_x{}^*$. When the reference current $i_x{}^* > 0$, the polarity of the terminal voltage distortion is negative, while $i_x{}^* < 0$, that is positive.

For ease analysis, the duration of voltage distortion is called "fault section" for short here. Based on (7), the relationships among the voltage distortions, currents reference polarity, and phase current can be obtained as shown in Table I.

From Table I, it can be noticed that when open-winding fault happens, its voltage distortions present two polarities according to reference current polarity. Through further analysis, three laws can be derived:

1) When winding x opens, faulty phase current is zero ($i_x = 0$), and the polarity of voltage distortions (Δ_{uxo}) is opposite to that of the reference current ($i_x{}^*$).
2) No matter which winding opens, the terminal voltage distortion has two polarities ("+" and "–"), i.e., fault has two subsections.
3) During winding open faults, fault section lasts for the whole electric cycle. While each subsection accounts for half of the electric cycle.

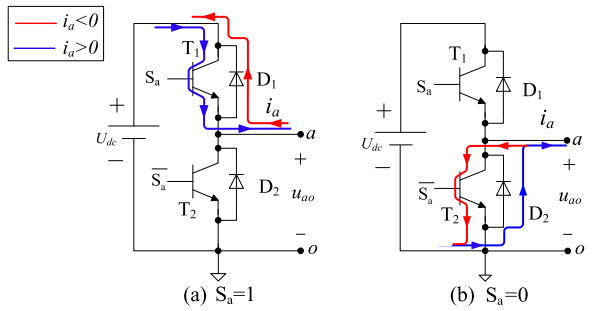

Fig. 3. Direction of i_a under normal condition.

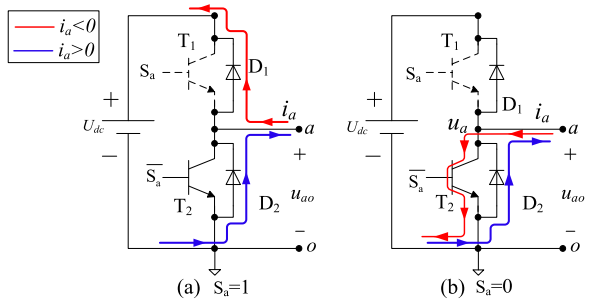

Fig. 4. Direction of i_a under switch T_1 open fault.

TABLE II
FAULTY PHASE TERMINAL VOLTAGE UNDER DIFFERENT CONDITIONS

Conditions	S_a=0, $i_a>0$	S_a=0, $i_a<0$	S_a=1, $i_a>0$	S_a=1, $i_a<0$
Normal	$u_{ao}=0$	$u_{ao}=0$	$u_{ao}=U_{dc}$	$u_{ao}=U_{dc}$
T_1 open	$u_{ao}=0$	$u_{ao}=0$	$u_{ao}=0$	$u_{ao}=U_{dc}$

B. Features of Open-Switch Fault

To distinguish the open-winding and open-switch faults, it is necessary to analyze the features of open-switch fault as well. Here, the open-fault in switch T_1 is taken as an example to analyze. The paths of phase current i_a under healthy and open-fault conditions are described in Figs. 3 and 4, respectively.

In the figures, the red and blue lines indicate the current flowing out of and into winding, respectively. S_a indicates switch state. When $S_a = 1$, switch T_1 is open. While $S_a = 0$, switch T_1 is close.

Comparing Figs. 3 and 4, it can be found that open-switch fault leads to the changes of current path and terminal voltage. The terminal voltage in the fault phase can be obtained as shown in Table II.

From Table II, it can be noticed that if $i_a > 0$ and $S_a = 1$, the terminal voltage distortion only exists in the section that the phase current is positive and fault-switch is ON.

Similarly, according to (5) the terminal voltage distortion under switch T_1 open fault can be written as follows:

$$\Delta u_{ao} = \begin{cases} -\frac{3(u^*_{an}-e_a)}{2}, & \text{when } i^*_a > 0 \\ 0, & \text{when } i^*_a < 0. \end{cases} \tag{8}$$

TABLE III
RELATIONSHIPS AMONG PMSM KEY VARIABLES DURING SWITCH FAULTS

Faulty switch	Voltage Distortion	Reference current polarity during fault section	Phase current
T_1	$\Delta u_{ao}<0$	$i_a{}^*>0$	$i_a=0$
T_2	$\Delta u_{ao}>0$	$i_a{}^*<0$	$i_a=0$
T_3	$\Delta u_{bo}<0$	$i_b{}^*>0$	$i_b=0$
T_4	$\Delta u_{bo}>0$	$i_b{}^*<0$	$i_b=0$
T_5	$\Delta u_{co}<0$	$i_c{}^*>0$	$i_c=0$
T_6	$\Delta u_{co}>0$	$i_c{}^*<0$	$i_c=0$

The terminal voltage distortions during open-switch fault can be generally expressed as follows:

$$\Delta u_{xo} = \begin{cases} -\frac{3(u^*_{xn}-e_x)}{2}, & \text{when } (-1)^{k+1}\cdot i^*_x > 0 \\ 0, & \text{when } (-1)^{k+1}\cdot i^*_x < 0 \end{cases} \tag{9}$$

where the superscript $k\in\{1, 2\}$, 1 and 2 denote upper and lower switches, respectively.

According to (9), the relationships among faulty switch, voltage distortion, reference current polarity, and phase current can be obtained as shown in Table III.

From Table III, two laws can be derived.

1) When a switch opens, its fault section can be determined by current reference polarity. It only takes up half of electric cycle.
2) Voltage distortion only exists in half of electric cycle. The polarity of terminal voltage distortion of upper switch open-fault is negative, while it is positive in lower switch open fault.

Through analysis, the similarity and difference of open-switch fault and open-winding fault can be extracted.

The similarity is that they may cause terminal voltage distortion, and the distortion is related to the phase current reference of the faulty phase.

The difference between these two faults lies in the fault section and terminal voltage distortion polarity. In open-winding fault, the fault section lasts the whole electric cycle. Therefore, the terminal voltage distortion has both positive and negative polarities, after changing current reference polarity. While in the open-switch fault, the terminal voltage distortion only has one polarity ("+" or "−").

III. FAULT DISTINGUISH AND LOCATION

Through above analysis, it can be noticed that open-winding and open-switch faults have similarity and difference. Their similarity mainly lies in voltage distortion magnitude, which can be used for fault detection. While their difference consists of distortion polarity and fault section, which can be applied for distinguishing.

A. Residuals Extraction and Residuals Modular

Motor fault leads to terminal voltage and phase current distortions simultaneously. The voltage and current distortions can be monitored by observer. However, conventional observer is sensitive to motor operating condition, which may lead to misdiagnosis. Considering that the differential observer possesses

superior robustness, it is employed in this paper [31]. Its analysis and design will not be described here.

According to paper [31], the improved residuals can be described as follows:

$$\begin{bmatrix} r_1(\mathrm{m}+1) \\ r_2(\mathrm{m}+1) \\ r_3(\mathrm{m}+1) \end{bmatrix} = (G - L_r) \cdot \begin{bmatrix} r_1(\mathrm{m}) \\ r_2(\mathrm{m}) \\ r_3(\mathrm{m}) \end{bmatrix} + H \cdot \begin{bmatrix} \Delta u_1(\mathrm{m}) \\ \Delta u_2(\mathrm{m}) \\ \Delta u_3(\mathrm{m}) \end{bmatrix} \quad (10)$$

where r_1, r_2, r_3 are differential current distortions postfault, $[r_1, r_2, r_3] = [\Delta i_a\text{–}\Delta i_b, \Delta i_b\text{–}\Delta i_c, \Delta i_c\text{–}\Delta i_a]$, $\Delta i_x = i_x^*\text{-}i_x$ is the difference between reference and actual currents, $G = \mathrm{gE}$, $H = \mathrm{hE}$, $g = \exp\{-R_s\mathrm{T_s}/(L\text{–}M)\}$, $h = (1\text{–}g)/R_s$, R_s is the phase resistance, L is three-phase self-inductances, M is phase mutual-inductances, E is the identity matrix, T_s is the current sampling period, m is the iteration number, L_r is the feedback coefficient, Δu_1, Δu_2, Δu_3 are the differential voltage distortion postfault, $[\Delta u_1, \Delta u_2, \Delta u_3] = [\Delta u_{ao}\text{-}\Delta u_{bo}, \Delta u_{bo}\text{-}\Delta u_{co}, \Delta u_{co}\text{-}\Delta u_{ao}]$, respectively.

The closed-loop pole of the observer can be derived as follows:

$$p_c = e^{-\frac{R_s T}{L-M}} - L_r = p_o - L_r \quad (11)$$

where p_c and p_o is the closed-loop and open-loop poles of the observer, respectively.

It is well known that feedback coefficient L_r plays an important role in close-loop observer and it can be determined according to the pole. In order to ensure the stability of the observer, p_0 should be set within unit circle in z-plane and the closed-loop poles should be assigned to 3–10 times faster than open-loop poles.

The PMSM is approximately three-phase symmetrical, the three feedback coefficients in feedback coefficient matrix can be selected equal for simplicity.

Normally, voltage distortions are very small, thus the induced residuals can be neglected. When fault occurs, the residual increases distinctly due to the voltage distortion.

To measure the residual magnitude, its modular is calculated as follows:

$$M_r = \sqrt{r_1^2 + r_2^2 + r_3^2} \quad (12)$$

where M_r is the residuals modular. Once the current RESIDUAL exceeds the threshold, the fault can be determined.

B. Adaptive Threshold for Fault Detection

It can be found that residuals amplitude varies with the change of motor current and voltage. As a result, fixed thresholds may lead to misdiagnosis. A simple and adaptive threshold is necessary.

Normally, motor three-phase current can be expressed as follows:

$$i_{abc} = I_m \sin(\omega t + \boldsymbol{\varphi}) \quad (13)$$

where I_m is the current amplitude, ω is the angular speed, φ is the initial phase angle, $\varphi = [0, -2\pi/3, 2\pi/3]^{\mathrm{T}}$, respectively.

When open-winding fault occurs in phase A, (13) can be rewritten as follows:

$$\begin{cases} i_a = 0 \\ i_b = \sqrt{3}\mathrm{I}_m \left[\sin\left(\omega t - \frac{2}{3}\pi\right) + \frac{1}{2}\sin\omega t\right] \\ i_c = \sqrt{3}\mathrm{I}_m \left[\sin\left(\omega t + \frac{2}{3}\pi\right) + \frac{1}{2}\sin\omega t\right]. \end{cases} \quad (14)$$

In order to understand the variation law of the residual amplitude, residuals modular should be calculated.

Substituting (13) and (14) into (12)

$$M_r = I_m \cdot \sqrt{\frac{9}{2} + \left(\frac{27}{2} - 9\sqrt{3}\right)\cos^2\omega t}. \quad (15)$$

From (15), it can be noticed that residuals can be expressed as a periodic signal which relate to actual current.

According to the analysis carried out in [31], residual relates to $\boldsymbol{i}$and $\Delta\boldsymbol{i}$, which can be expressed as follows:

$$M_r < m_1 \cdot ||i||_2 + m_2 \cdot ||\Delta i||_2 \quad (16)$$

where m_1, m_2 are parameters which heavily rely on model errors, detailed definitions and settings are proved in [31], $|\cdot|$ is the absolute value symbol, $\Delta\boldsymbol{i}(k) = \Delta\boldsymbol{i}(k+1) - \boldsymbol{i}(k)$.

From (16), the residual amplitude can be eventually expressed as an equation related to the actual current.

Combining (15) and (16), the threshold value is set as follows:

$$M_r = f_0 + f_1 \cdot i_s \quad (17)$$

where f_0 is a small positive constant to avoid noise interference, f_1 is the coefficient of i_s. $i_s = \sqrt{i_\alpha^2 + i_\beta^2}$, which is the actual motor current amplitude, and I_α, i_β is current in the coordinate system.

According to inverse Clark transform, the motor *abc* currents can be transformed as follows:

$$[i_a i_b i_c]^T = T_{3s/2s}^{-1}[i_\alpha i_\beta]^T \quad (18)$$

where $T_{3s/2s}^{-1} = \frac{2}{3}\begin{bmatrix} 1 & 0 \\ -\frac{1}{2} & \frac{\sqrt{3}}{2} \\ -\frac{1}{2} & -\frac{\sqrt{3}}{2} \end{bmatrix}$.

And then, differential current can be expressed by $\alpha\beta$ current

$$\begin{cases} i_a - i_c = \frac{\sqrt{3}}{2}\left(i_\beta + \sqrt{3} i_\alpha\right) \\ i_b - i_a = \frac{\sqrt{3}}{2}\left(i_\beta - \sqrt{3} i_\alpha\right). \end{cases} \quad (19)$$

Calculating the squares sum of the differential currents in (19), the fault indicator can be represented as follows:

$$\mathrm{FI} = \sqrt{(i_a - i_c)^2 + (i_b - i_a)^2} = \frac{\sqrt{3}}{2}\sqrt{2i_s^2 + 4i_\alpha^2} \quad (20)$$

where FI is fault indicator changes with motor operating condition. When fault occurs, i_s and i_α decrease. Hence, FI shows a decreasing trend, which effectively avoids misdiagnosis.

Finally, the simplified adaptive threshold can be defined as follows:

$$T_h = f_0' + f_1 \cdot FI \quad (21)$$

where T_h is the designed adaptive threshold, f_0' is a small positive constant to avoid noise interference, f_1 is the coefficient of FI, which is set according to the model error and the operation of the motor, respectively.

To avoid false alarm caused by random error, f_0' can be set to 6–12 times of standard deviation. f_1 is set to 2–3 times to the critical value which is tested under parameters variation (motor resistance and inductance vary 30% and 50%, respectively).

C. Simple Faulty Phase Identification Method

According to Section II, the fault section and terminal voltage distortion polarity of these two kinds of faults are different, which can be employed for distinguishing.

In (10), since the three feedback coefficients in feedback coefficient matrix is equal, the residual responses would be same for the same voltage distortion inputs. Once open-switch fault or open-winding fault occurs, Δu_1, Δu_2, Δu_3 always perform as one of them is always close to 0, and the other two change symmetrically. Therefore, one of the three current residuals r_1, r_2, r_3 is always close to 0, and the other two residuals are equal in magnitude and opposite in polarity. Considering that the residual amplitude varies with the motor operating condition which may cause false diagnosis, current residuals are normalized as $\boldsymbol{r_n} = \boldsymbol{r}/M_r$. Taking switch T_1 open fault as an example and neglecting the effects of noise, the normalized residual vector of switch T_1 open-fault can be written as $[r_1,\ r_2,\ r_3]/\sqrt{r_1^2+r_2^2+r_3^2} = (-1,0,1)/\sqrt{2}$. Other faults can be analyzed similarly.

For ease analysis, the normalized vector obtained from ideal condition is called "template vector." The template vector under different open-switch fault can be expressed as $\boldsymbol{a_{1-6}}$, where, $\boldsymbol{a_{1-6}}$ = [–10,1], [10,–1], [1,–10], [–11,0], [01,–1], [0,–11], respectively.

However, in the actual situation, the normalized vector is not exactly equal to the template vector due to noise and other factors. In order to locate the fault, actual normalized vector needs to be matched to template vectors.

According to the minimum distance principle, when the normalized residual vector is close to the template vector, the fault can be located

$$||\mathrm{r_n} - \mathrm{a_D}|| = \min_{n\in\{1,2,3,4,5,6\}} (||\mathrm{r_n} - \mathrm{a_n}||_2) \tag{22}$$

where the subscript D is used to record the subscript of template vector which is closest to the normalized vector.

The faulty source, reference current polarity in fault section and normalized residual vectors matched to template vector are listed in Table IV.

From Table IV, it can be noticed that there are six different direction-fixed vector $\boldsymbol{a_1}^{\mathrm{T}}$–$\boldsymbol{a_6}^{\mathrm{T}}$. Combined with D, the faulty phase can be located

$$F_p = \lceil D/2 \rceil \tag{23}$$

where $\lceil\cdot\rceil$ is top integral function, F_p is the faulty phase indicator, F_p = 1, 2, 3 corresponding to the fault phase A, B, C, respectively.

For open-switch fault, each vector corresponds to a certain fault source. As to the open-winding fault, there are two different vectors corresponding to same phase. On the other hand, a vector would correspond to open-switch fault or open-winding fault, which may lead to misdiagnosis. Hence, the fault cannot be located accurately just according to the vector matching. Further analysis is still necessary for distinguishing.

TABLE IV
NORMALIZED RESIDUAL VECTORS

Faulty Source	Reference current polarity in fault section	Normalized residual vector
T_1	$i_a^* > 0$	$\boldsymbol{a_1}^{\mathrm{T}} = (-1,0,1)/\sqrt{2}$
T_2	$i_a^* < 0$	$\boldsymbol{a_2}^{\mathrm{T}} = (1,0,-1)/\sqrt{2}$
T_3	$i_b^* > 0$	$\boldsymbol{a_3}^{\mathrm{T}} = (1,-1,0)/\sqrt{2}$
T_4	$i_b^* < 0$	$\boldsymbol{a_4}^{\mathrm{T}} = (-1,1,0)/\sqrt{2}$
T_5	$i_c^* > 0$	$\boldsymbol{a_5}^{\mathrm{T}} = (0,1,-1)/\sqrt{2}$
T_6	$i_c^* < 0$	$\boldsymbol{a_6}^{\mathrm{T}} = (0,-1,1)/\sqrt{2}$
Winding A	$i_a^* > 0$	$\boldsymbol{a_1}^{\mathrm{T}} = (-1,0,1)/\sqrt{2}$
	$i_a^* < 0$	$\boldsymbol{a_2}^{\mathrm{T}} = (1,0,-1)/\sqrt{2}$
Winding B	$i_b^* > 0$	$\boldsymbol{a_3}^{\mathrm{T}} = (1,-1,0)/\sqrt{2}$
	$i_b^* < 0$	$\boldsymbol{a_4}^{\mathrm{T}} = (-1,1,0)/\sqrt{2}$
Winding C	$i_c^* > 0$	$\boldsymbol{a_5}^{\mathrm{T}} = (0,1,-1)/\sqrt{2}$
	$i_c^* < 0$	$\boldsymbol{a_6}^{\mathrm{T}} = (0,-1,1)/\sqrt{2}$

D. Fault Location

From (5), (7) and (9), it can be found that through changing current reference polarity, the residual vector can be changed accordingly in open-winding fault. However, this phenomenon does not exist in open-switch fault. Therefore, the fault type can be distinguished by controlling the current reference polarity.

According to (5), current reference polarity can be reversed by changing the phase voltage reference

$$u_x = u_{xn}^* - e_x \tag{24}$$

where u_x is the sum of reference voltage drop on the winding resistance and inductances of phase x.

Generally, $u_{xn}{}^*$ is set approaching e_x to reduce the motor loss. Here, it is artificially changed for varying the direction of $i_x{}^*$ as soon as possible. Thus, the new voltage reference $u_x{}^*$ is given as follows:

$$\begin{aligned} u_x' &= (u_{xn}^*)' - e_x = (u_{xn}^*)' - u_{xn}^* + u_{xn}^* - e_x \\ &\approx (u_{xn}^*)' - u_{xn}^* \end{aligned} \tag{25}$$

where u_x' denotes the revised variables, and $(u_{xn}{}^*)$' is the new modified phase voltage reference, respectively.

Here, the new $u_{xn}{}^*$ is designed as follows:

$$(u_{xn}^*)' = \lambda u_{xn}^* \tag{26}$$

where λ is the linear coefficient.

Substituting (26) into (25), the relationship between $(u_x{}^*)$'and $u_{xn}{}^*$ can be derived as follows:

$$\begin{aligned} (u_x^*)' &= (\lambda - 1)\, u_{xn}^* \\ \operatorname{sign}\left((u_x^*)'\right) &= \operatorname{sign}((\lambda-1)) \cdot \operatorname{sign}(u_x^*). \end{aligned} \tag{27}$$

In order to change the direction of the current residual as soon as possible, the phase current reference should be set as a large negative value, and λ should be set as a large value. While, if the value of λ is too large, the torque would reduce significantly. Notice that the torque fluctuations caused by the voltage modification should be smaller than that caused by open-switch fault and open-winding fault. However, a smaller λ may lead to longer time for inverting residual polarity. The absolute value of λ should be set smaller than 1.

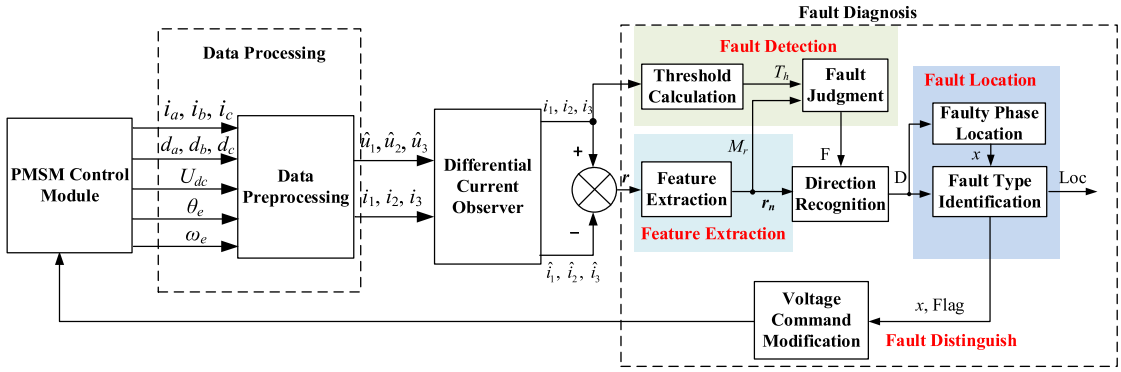

Fig. 5. Diagram of the proposed fault diagnosis method.

It can be found that the transfer function from voltage to current is a first inertial element. The smaller the time constant, the faster the response. For individual motors, their difference mainly lies in inductance and resistance values. If the inductance and resistance values are larger, its current response would be slow. Hence, it is necessary to choose a larger λ. In contrast, smaller λ should be set for motors with small inductance and resistance. In this article, λ∈ (–0.35, –0.25) is a suitable range obtained by experiments.

Notice that the modification of phase voltage reference (27) cannot be directly implemented on the PMSM control system. To realize the modification, the reference voltage should be transferred to the $\alpha\beta$ coordinate system

$$[u_{an}^* u_{bn}^* u_{cn}^*]^T = T_{3s/2s}^{-1}\left[u_\alpha^* u_\beta^*\right]^T \tag{28}$$

$$\left[(u_\alpha^*)'(u_\beta^*)'\right]^T = T_{3s/2s}\left[(u_{an}^*)'(u_{bn}^*)'(u_{cn}^*)'\right]^T \tag{29}$$

where $T_{3s/2s} = \frac{2}{3}\begin{bmatrix}1 & -\frac{1}{2} & -\frac{1}{2}\\ 0 & \frac{\sqrt{3}}{2} & -\frac{\sqrt{3}}{2}\end{bmatrix}$, $u_\alpha{}^*, u_\beta{}^*$ $(u_\alpha{}^*)', (u_\beta{}^*)'$ are voltage reference and new modified voltage reference under the $\alpha\beta$ coordinate system, respectively.

The relationship between the new modified voltage reference and the original voltage reference is expressed as follows:

$$[(u_a^*)'(u_\beta^*)'] = P \cdot [u_a^* u_\beta^*] \tag{30}$$

where P is the new transformation matrix. $P = [(0.5–\lambda)/30;01]$, $[5–\lambda/6, \sqrt{3}\,(1+\lambda)/6; \sqrt{3}\,(1+\lambda)/6, 1–\lambda/2]$, $[5–\lambda/6, \sqrt{3}\,(1+\lambda)/6; -\sqrt{3}\,(1+\lambda)/6, 1–\lambda/2]$, respectively.

Once a revised residual vector is recognized, the system can be judged as open-winding fault. Otherwise, the open-switch fault is judged. At this instant, the modification of phase voltage reference can be stopped. And then, the fault diagnosis system outputs the fault source indicator (L_{oc}). L_{oc} definition is shown in Table V.

It can be noticed that terminal voltage distortion is proportional to phase current reference in star-connected motor. The terminal voltage distortion polarity and current residuals can be inverted by changing the polarity of the phase current. While in delta-connected motor, the faulty phase terminal voltage distortion relates to faulty phase current reference and terminal voltage distortion of other phase. The polarity of terminal voltage distortion and current residuals cannot be inverted by changing the direction of the phase current alone. Hence, this reference voltage correction-based fault cannot be used directly in delta-connected motors.

TABLE V
L_{OC} DEFINITION

Value		Fault Source	Fault Type
$L_{oc}=0$	Flag = 0	No fault	--
	Flag = 1	Undetermined	Undetermined
$L_{oc}=1$–6		Switch T_{Loc}	Open-switch fault
$L_{oc}=7$		Winding A	Open-winding fault
$L_{oc}=8$		Winding B	
$L_{oc}=9$		Winding C	

Fig. 5 shows the diagram of the proposed fault diagnosis method. It mainly includes four modules, PMSM control module, data processing module, differential currents observer module, and fault diagnosis module. The data processing module is used for collecting motor real-time variables and preprocessing them. And then, the processed data are put into differential current observer to obtain the estimated differential current. In the fault diagnosis module, the difference between the estimated and actual currents is used for residual calculation. Residual magnitude M_r and normalized residual vector $\boldsymbol{r_n}$ are obtained in feature extraction module. After that, the residual is compared with threshold. If residual is greater than the threshold, the system can be determined as faulty, and $\boldsymbol{a_{1-6}}$ can be matched. Then, the reference voltage is changed to locate the fault. If $\boldsymbol{r_n}$ changes to another vector of same phase as shown in Table IV, open-winding fault can be determined. If it changes to zero, open-switch fault can be determined. Consequently, combing with the variable **D,** open-switch fault and open-winding fault can be distinguished and located.

Note that it takes time for current response after the voltage reference modified. Thus, waiting time should be reserved. Considering that motor can be regarded as first-order system, the waiting time can be set as 1–2 times of its inertial time constant.

IV. PMSM Control System Experiments

A. Experiment Setup

Sufficient experiments have been conducted on PMSM platform as shown in Fig. 6. The digital signal processor (DSP

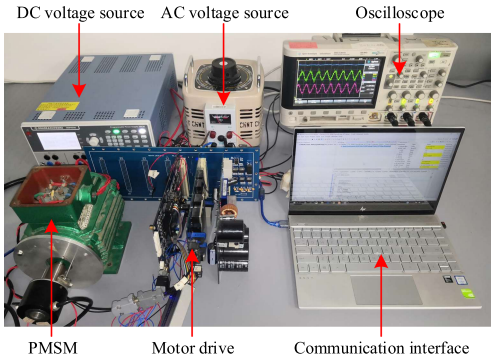

Fig. 6. PMSM experimental platform.

TABLE VI
PMSM CONTROL SYSTEM PARAMETERS

Parameters	Unit	Value
Rated Power	W	120
Rated Current	A	3.14
Rated Output Torque	N·m	1.1
Rated Rotor Speed	rpm	1000
Flux Linkage	Wb	0.13
Phase Resistance	Ω	0.67
Phase Inductance	mH	3.1
Mutual Inductance	mH	1.5
Pole Pairs	—	2
DC Bus Voltage	V	100
PWM Frequency	kHz	20
Current Sampling Time	s	5×10^{-5}

TABLE VII
PARAMETERS OF THE FAULT DIAGNOSIS ALGORITHM

Parameters	Symbol	Value
Threshold parameters	f_0	0.2
	f_1	0.15
Linear coefficient	λ	−0.3

TMS320F28335) is used for motor control and fault diagnosis. Motor rotor position is detected by a 12-bit absolute encoder. Hall current sensors are used to measure motor phase currents. The integrated power module inverter circuit is used for driving. The motor load is provided by a magnetic powder brake. The main parameters of the motor system are listed in Table VI.

In the experiment, the open-switch fault and open-winding fault are given by software. For the former fault, pulsewidth modulation (PWM) duty cycle of the fault switch is set as 0. As for the latter fault, it is realized by disconnecting the relay between the winding and inverter. Parameters used in the fault diagnosis algorithm are given in Table VII.

B. Experiment I: Open-Switch Fault Test

First, the effectiveness of the proposed open-switch fault detection and location method is verified. In this experiment, PMSM operates at 500 r/min with 0.11 N·m load (10%), and switch T_2 opens at 0.15 s. With these settings, detailed experiments are conducted.

Experiment results are reported in Fig. 7. From Fig. 7(a) and (b), it can be seen that the current in phase A changes from sinusoidal-wave to half-wave at the instant of fault, and its voltage distorts immediately. And then, according to the reference and actual phase currents, the residual magnitude M_r and the adaptive threshold T_h can be calculated [(12) and (21)]. As illustrated in Fig. 7(c) and (d), residuals (r_1, r_2, r_3) are close to 0, and the residuals modular M_r is far below the threshold prefault. When open-switch fault occurs at $t = 0.15$ s, the residuals modular M_r rises rapidly and exceeds the threshold. The normalized residual vector $\boldsymbol{r}_\mathbf{n}$ is $(1, 0, -1)/\sqrt{2}$ during the fault [see Fig. 7(c)], which is consistent with Table IV. Therefore, the fault can be located at phase A, which is consistent with Table V.

And then, modifying the terminal voltage reference according to (26), a sudden-jump in phase currents and terminal voltage presents as shown in Fig. 7(a) and (b) (dashed circles). As a result, the value of indicator variable **D** changes from 1 to 0 accordingly [see Fig. 7(e)]. This means the modification of voltage reference can change the current and residual vector simultaneously. This character can be employed for distinguishing the faults. After that, switch T_2 open fault can be judged and fault source indicator $L_{oc} = 2$ can be obtained according to Table V [see Fig. 7(e)].

In this experiment, the fault can be detected within 0.1504 s, and can be located within 0.1515 s. It takes 5% of an electric cycle to realize fault detection and location. The experiment result is consistent with the analysis conducted in Section III.

C. Experiment II: Open-Winding Fault Test

Second, the effectiveness of the proposed open-winding fault detection and location method is verified. In this experiment, PMSM operates at 500 r/min with 0.11 N·m load, and winding A opens at 0.15 s. With these settings, detailed experiments are developed.

Experiment results are shown in Fig. 8. It can be seen that the current in phase A changes from sinusoidal-wave to zero at the instant of faut, and its voltage distorts immediately [see Fig. 8(a) and (b)]. Before the fault, residuals (r_1, r_2, r_3) is close to 0 and residuals modular M_r is below the threshold [see Fig. 8(c) and (d)]. When the winding A opens at 0.15 s, the residuals modulus rises rapidly and exceeds the threshold at $t = 0.1505$ s. At this instant, the normalized residual vector $\boldsymbol{r}_\mathbf{n}$ is $(1, 0, -1)/\sqrt{2}$ and the indicator variable **D** is directed to 2 [see Fig. 8(e)]. Therefore, the fault can be located at phase A.

And then, the terminal voltage reference is modified according to (26). At this instant, residual vector $\boldsymbol{r}_\mathbf{n}$ changes to the opposite direction $(-1, 0, 1)/\sqrt{2}$, and the indicator vector varies from 2 to 1. Therefore, winding A open fault can be judged and fault source indicator $L_{oc} = 7$ [see Fig. 8(f)]. In this experiment, the fault is located at $t = 0.15155$ s. It takes 1.4 ms to detect and locate the fault (5.2% of electric cycle). This experiment result is consistent with the analysis conducted in Section III.

With the proposed method, the open-switch and open-winding faults can be diagnosed within 5% of the electric cycle.

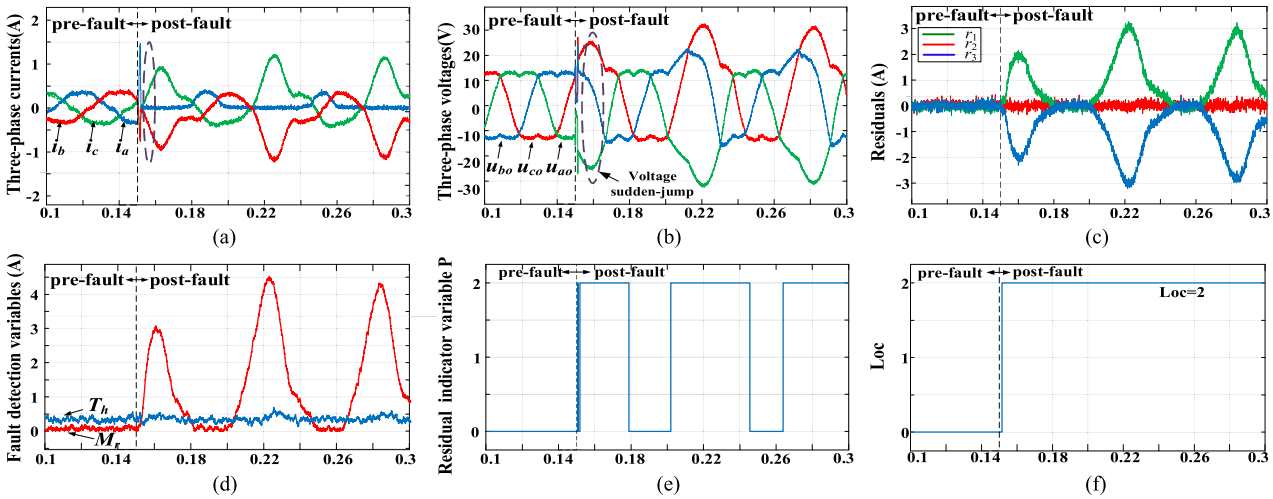

Fig. 7. Switch T_2 open-fault diagnosis waveforms. (a) Three-phase currents. (b) Three-phase voltages. (c) Residual components. (d) Fault detection index and threshold. (e) Residual direction. (f) Fault source.

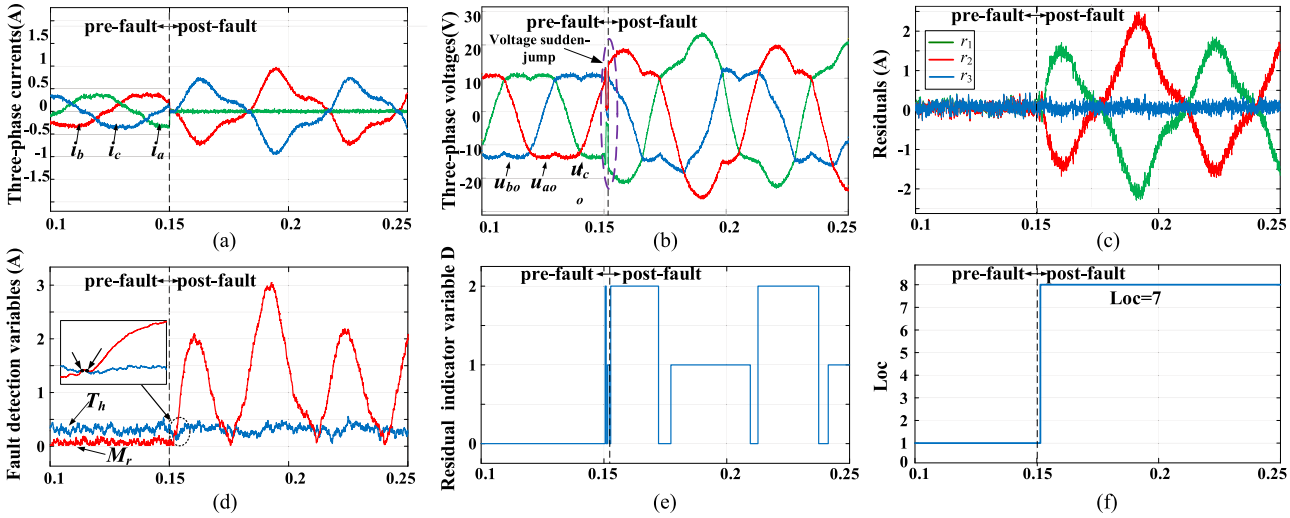

Fig. 8. Winding A open-fault diagnosis waveforms. (a) Three-phase currents. (b) Three-phase voltages. (c) Residual components. (d) Fault detection index and threshold. (e) Residual direction. (f) Fault source.

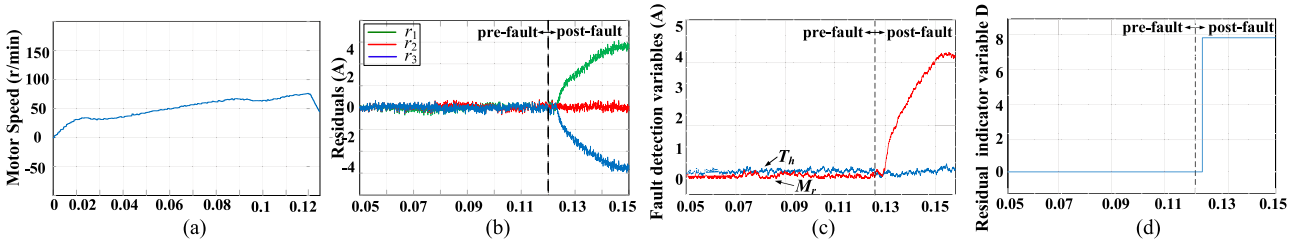

Fig. 9. Effectiveness test of the proposed method during motor acceleration. (a) Motor speed. (b) Residual components. (c) Fault detection index and threshold variables. (d) Fault source.

D. Experiment III: Robustness Test Under Variable Speed and Torque Condition

In order to verify the robustness of the proposed method, it is tested during motor acceleration, deceleration, and torque step, respectively.

First, the motor is controlled accelerating from 0 and decelerating from 1000 r/min with 0.11 N·m load, respectively. The winding A opens at $t = 0.12$ s during motor acceleration and opens at $t = 0.15$ s during motor deceleration. Experimental results are shown in Figs. 9 and 10, separately. As shown in Figs. 9(a) and 10(a), open-winding fault leads to motor speed fluctuations no matter it is accelerating or decelerating. Normally, speed variation has little effect on the amplitude of the residual components [see Figs. 9(b) and 10(b)]. While, the threshold amplitude changes with the speed

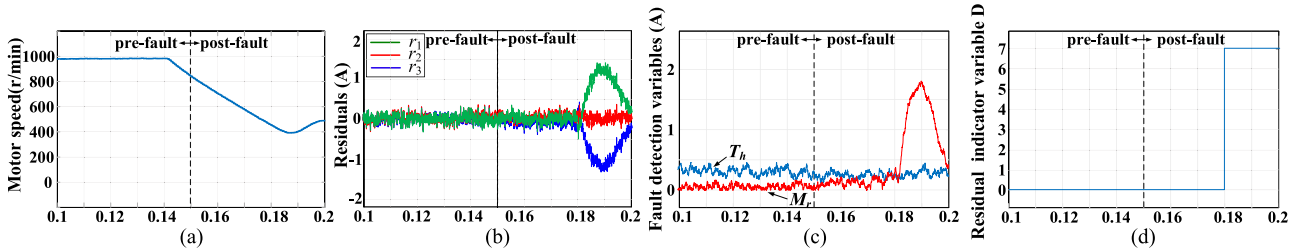

Fig. 10. Effectiveness test of the proposed method during motor deceleration. (a) Motor speed. (b) Residual components. (c) Fault detection index and threshold variables. (d) Fault source.

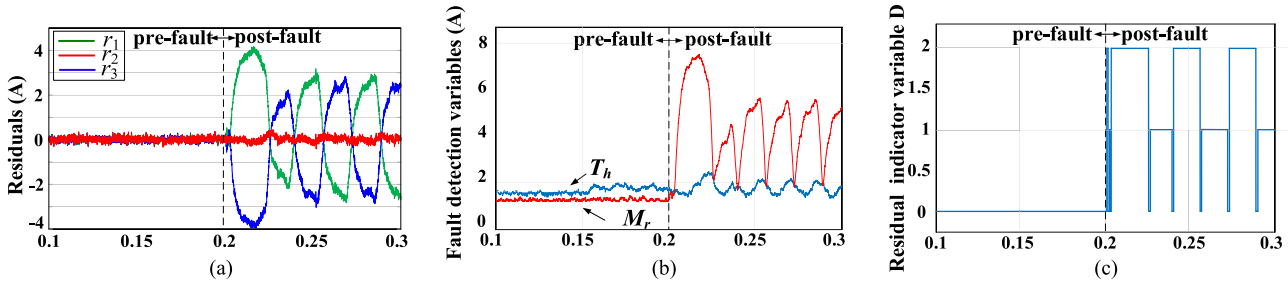

Fig. 11. Effectiveness test of the proposed method during torque step. (a) Residual components (b) Fault detection index and threshold variables. (c) Residual direction.

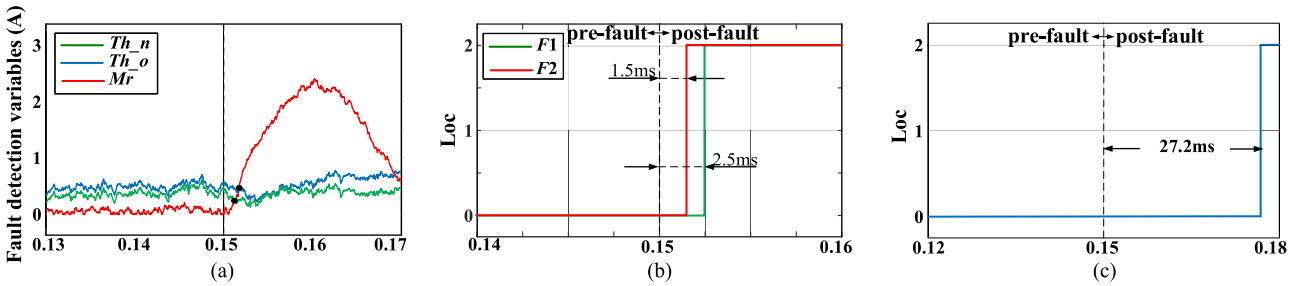

Fig. 12. Effectiveness comparison between the original threshold and proposed threshold. (a) Fault detection index and threshold. (b) Fault detection result comparison (F1 and F2 corresponding to original method and proposed method, respectively). (c) Localization time without using voltage correction-based algorithm.

variation [see Figs. 9(c) and 10(c)] and the designed threshold T_h is higher than index M_r. After open-winding fault occurs, T_h declines significantly and it is lower than Mr. Due to the self-adjusting characteristics of the designed threshold, no false detection or missed detection presents under different operation conditions.

Hence, accurate fault detection and location can be yielded as illustrated in Figs. 9(d) and 10(d).

And then, torque step is set, $T_e^* = 0.11$ N·m before $t = 0.15$ s and $T_e^* = 0.55$ N·m after $t = 0.15$ s. The open-winding fault occurs at 0.2 s. The experiment results are shown in Fig. 11. It can be seen M_r is always below the threshold T_h before fault occurs even when the torque changes [see Fig. 11(b)]. After open-winding fault occurs, residuals amplitude rises and exceeds threshold. According to Fig. 11(c), fault can be located at phase A.

E. Experiment IV: Comparison With Conventional Method

Finally, the performance of the proposed adaptive threshold is compared with that of the threshold proposed in paper [31] which possesses fast detection speed and good robustness (called original threshold for simplicity). In this experiment, PMSM operates at 500 r/min with 0.11 N·m load, and switch T_2 opens at 0.15 s. The corresponding experiment results are described in Fig. 11. Here, *th_n* and *th_o* in Fig. 12(a) denote proposed threshold and original threshold, respectively.

From Fig. 12(a) it can be seen that the proposed threshold is slightly lower than the original threshold before fault. When fault occurs, these two thresholds show a decreasing trend. The proposed threshold decreases faster than the original thresholds. The fault detection index indicates that the diagnosis time of the proposed threshold is reduced by almost 1 ms compared

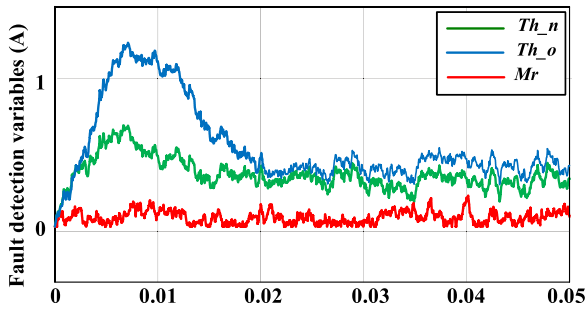

Fig. 13. Start-up comparison between the original threshold and proposed threshold.

TABLE VIII
OPEN-FAULT DETECTION TIMES IN THE EXPERIMENTS

Methods	rapidity
Proposed method	1.5 ms
Conventional method	2.5 ms

to the original threshold [see Fig. 12(b)]. Fig. 12(c) shows the localization time without varying the reference voltage polarity. It takes longer time to locate the fault.

Fig. 13 shows that there is a sudden change in the residuals during motor start-up. This phenomenon may lead to incorrect diagnosis. Compared to the original threshold, the proposed threshold possesses faster rise rate. Therefore, the incorrect diagnosis exists in original method during motor start-up can be avoided.

For quantitative comparison, the fault detection times of these two methods are listed in Table VIII. The proposed method shows rapidity compared with the conventional method.

V. CONCLUSION

Open-winding and open-switch fault would degrade motor performance seriously. However, their similar postfault current behavior makes it difficult to distinguish them, and misdiagnosis often occurs. False detection and localization may lead to motor damage. To overcome this problem, a novel faults detection and distinguish method is proposed in this article. First, by analyzing the law of current residuals caused by open-switch fault and open-winding fault, respectively, an adaptive threshold is designed. Compared with existing methods, it is simple but has great robustness, which improves diagnostic speed and accuracy. And then, based on the different features of these two types of faults and the relationship between voltage distortion and current reference, a fault distinguishment method is designed. It is realized by modifying voltage reference. This method greatly shorten fault distinguish and locate time compared to the existing methods. Moreover, it is simple to be implemented and easy to be adjusted.

The effectiveness and superiority of the proposed fault diagnosis method are verified on PMSM platform. The experimental results indicate that the proposed threshold possesses higher fault detection speed (within 5% of an electrical period) and accuracy compared with the conventional method. In addition, the location algorithm can locate faults within 6% of the electric cycle.

REFERENCES

[1] W. Wang, M. Cheng, B. Zhang, Y. Zhu, and S. Ding, "A fault-tolerant permanent-magnet traction module for subway applications," *IEEE Trans. Power Electron.*, vol. 29, no. 4, pp. 1646–1658, Apr. 2014.
[2] J. Fang, X. Zhou, and G. Liu, "Instantaneous torque control of small inductance brushless DC motor," *IEEE Trans. Power Electron.*, vol. 27, no. 12, pp. 4952–4964, Dec. 2012.
[3] C. Wu, C. Guo, Z. Xie, F. Ni, and H. Liu, "A signal-based fault detection and tolerance control method of current sensor for PMSM drive," *IEEE Trans. Ind. Electron.*, vol. 65, no. 12, pp. 9646–9657, Dec. 2018.
[4] T. Orlowska-Kowalska et al., "Fault diagnosis and fault-tolerant control of pmsm drives-state of the art and future challenges," *IEEE Access*, vol. 10, pp. 59979–60024, 2022.
[5] Q. A. B. Tian, J. Duan, D. Semenov, D. Sun, and L. Sun, "Cancellation of torque ripples with FOC strategy under two-phase failures of the five-phase PM motor," *IEEE Trans. Power Electron.*, vol. 32, no. 7, pp. 5459–5472, Jul. 2017.
[6] M. Cheng, J. Hang, and J. Zhang, "Overview of fault diagnosis theory and method for permanent magnet machine," *Chin. J. Elect. Eng.*, vol. 1, no. 1, pp. 21–36, Dec. 2015.
[7] S. Yang, D. Xiang, A. Bryant, P. Mawby, L. Ran, and P. Tavner, "Condition monitoring for device reliability in power electronic converters: A review," *IEEE Trans. Power Electron.*, vol. 25, no. 11, pp. 2734–2752, Nov. 2010.
[8] B. Lu and S. K. Sharma, "A literature review of IGBT fault diagnostic and protection methods for power inverters," *IEEE Trans. Ind. Appl.*, vol. 45, no. 5, pp. 1770–1777, Sep./Oct. 2009.
[9] W. Zhang, D. Xu, P. Enjeti, H. Li, J. Hawke, and H. Krishnamoorthy, "Survey on fault-tolerant techniques for power electronic converters," *IEEE Trans. Power Electron.*, vol. 29, no. 12, pp. 6319–6331, Dec. 2014.
[10] W. Li, H. Tang, S. Luo, X. Yan, and Z. Wu, "Comparative analysis of the operating performance, magnetic field, and temperature rise of the three-phase permanent magnet synchronous motor with or without fault-tolerant control under single-phase open-circuit fault," *IET Electric Power Appl.*, vol. 15, no. 7, pp. 861–872, Mar. 2021.
[11] M. Salehifar, R. S. Arashloo, J. M. Moreno-Equilaz, V. Sala, and L. Romeral, "Fault detection and fault tolerant operation of a five phase PM motor drive using adaptive model identification approach," *IEEE Trans. Emerg. Sel. Topics Power Electron.*, vol. 2, no. 2, pp. 212–223, Jun. 2014.
[12] H. Mesai-Ahmed, I. Jlassi, A. J. M. Cardoso, and A. Bentaallah, "Multiple open-circuit faults diagnosis in six-phase induction motor drives using stator current analysis," *IEEE Trans. Power Electron.*, vol. 37, no. 6, pp. 7275–7285, Jun. 2022.
[13] W. Li, G. Feng, Z. Li, M. S. Toulabi, and N. C. Kar, "Extended kalman filter based inductance estimation for dual three-phase permanent magnet synchronous motors under the single open-phase fault," *IEEE Trans. Energy Convers.*, vol. 37, no. 2, pp. 1134–1144, Jun. 2022.
[14] J. Sun, C. Li, Z. Zheng, K. Wang, and Y. Li, "A generalized, fast and robust open-circuit fault diagnosis technique for star-connected symmetrical multiphase drives," *IEEE Trans. Energy Convers.*, vol. 37, no. 3, pp. 1921–1933, Sep. 2022.
[15] G. Yang, J. Yang, S. Li, and H. Hussain, "A simple and efficient strategy for online detection of multiple open-switch fault in multiphase machine drive systems," *IEEE Trans. Power Electron.*, vol. 37, no. 9, pp. 11058–11070, Sep. 2022.
[16] S. Yang, G. Chen, and D. Jian, "On-line stator open-phase fault detection and tolerant control for permanent magnet machines using the neutral point voltage," *IEEE Access*, vol. 5, pp. 1073–1082, 2017.
[17] X. Wuet al., "A fast and robust diagnostic method for multiple open-circuit faults of voltage-source inverters through line voltage magnitudes analysis," *IEEE Trans. Power Electron.*, vol. 35, no. 5, pp. 5205–5220, May 2020.
[18] Z. Li, H. Ma, Z. Bai, Y. Wang, and B. Wang, "Fast transistor open-circuit faults diagnosis in grid-tied three-phase vsis based on average bridge arm pole-to-pole voltages and error-adaptive thresholds," *IEEE Trans. Power Electron.*, vol. 33, no. 9, pp. 8040–8051, Sep. 2018.
[19] H. Henaoet al., "Trends in fault diagnosis for electrical machines: A review of diagnostic techniques," *IEEE Ind. Electron. Mag.*, vol. 8, no. 2, pp. 31–42, Feb. 2014.
[20] J. O. Estima and A. J. Marques Cardoso, "A new algorithm for real-time multiple open-circuit fault diagnosis in voltage-fed PWM motor drives by the reference current errors," *IEEE Trans. Ind. Electron.*, vol. 60, no. 8, pp. 3496–3505, Aug. 2013.

[21] S. Khojet, E. Khil, I. Jlassi, A. J. Marques Cardoso, J. O. Estima, and N. Mrabet-Bellaaj, "Diagnosis of open-switch and current sensor faults in PMSM drives through stator current analysis," *IEEE Trans. Ind. Appl.*, vol. 55, no. 6, pp. 5925–5937, Nov./Dec. 2019.
[22] A. Sapena-Bañó, M. Pineda-Sanchez, R. Puche-Panadero, J. Martinez-Roman, and D. Matić, "Fault diagnosis of rotating electrical machines in transient regime using a single stator current's FFT," *IEEE Trans. Instrum. Meas.*, vol. 64, no. 11, pp. 3137–3146, Nov. 2015.
[23] N. Wassinger, E. Penovi, R. G. Retegui, and S. Maestri, "Open-circuit fault identification method for interleaved converters based on time-domain analysis of the state observer residual," *IEEE Trans. Power Electron.*, vol. 34, no. 4, pp. 3740–3749, Apr. 2019.
[24] C. Yang et al., "Voltage difference residual-based open-circuit fault diagnosis approach for three-level converters in electric traction systems," *IEEE Trans. Power Electron.*, vol. 35, no. 3, pp. 3012–3028, Mar. 2020.
[25] Q. An, L. Sun, and L. Sun, "Current residual vector-based open-switch fault diagnosis of inverters in PMSM drive systems," *IEEE Trans. Power Electron.*, vol. 30, no. 5, pp. 2814–2827, May 2015.
[26] S. M. Jung, J. S. Park, H. W. Kim, K.-Y. Cho, and M.-J. Youn, "An MRAS-based diagnosis of open-circuit fault in PWM voltage-source inverters for PM synchronous motor drive systems," *IEEE Trans. Power Electron.*, vol. 28, no. 5, pp. 2514–2526, May 2013.
[27] W. Huang, J. Du, W. Hua, K. Bi, and Q. Fan, "A hybrid model-based diagnosis approach for open-switch faults in PMSM drives," *IEEE Trans. Power Electron.*, vol. 37, no. 4, pp. 3728–3732, Apr. 2022.
[28] I. Jlassi, J. O. Estima, S. Khojet El Khil, N. M. Bellaaj, and A. J. M. Cardoso, "Multiple open-circuit faults diagnosis in back-to-back converters of PMSG drives for wind turbine systems," *IEEE Trans. Power Electron.*, vol. 30, no. 5, pp. 2689–2702, May 2015.
[29] I. Jlassi, J. O. Estima, S. K. El Khil, N. M. Bellaaj, and A. J. M. Cardoso, "A robust observer-based method for IGBTs and current sensors fault diagnosis in voltage-source inverters of PMSM drives," *IEEE Trans. Ind. Appl.*, vol. 53, no. 3, pp. 2894–2905, May–Jun. 2017.
[30] H. Yin, Y. Chen, Z. Chen, and M. Li, "Adaptive fast fault location for open-switch faults of voltage source inverter," *IEEE Trans. Circuits Syst.*, vol. 68, no. 9, pp. 3965–3974, Sep. 2021.
[31] X. Zhou, J. Sun, P. Cui, Y. Lu, M. Lu, and Y. Yu, "A fast and robust open-switch fault diagnosis method for variable-speed PMSM system," *IEEE Trans. Power Electron.*, vol. 36, no. 3, pp. 2598–2610, Mar. 2021.
[32] Z. Gao, C. Cecati, and S. X. Ding, "A survey of fault diagnosis and fault-tolerant techniques—Part I: Fault diagnosis with model-based and signal-based approaches," *IEEE Trans. Ind. Electron.*, vol. 62, no. 6, pp. 3757–3767, Jun. 2015.
[33] K. Choi, Y. Kim, S. - K. Kim, and K.-S. Kim, "Current and position sensor fault diagnosis algorithm for PMSM drives based on robust state observer," *IEEE Trans. Ind. Electron.*, vol. 68, no. 6, pp. 5227–5236, Jun. 2021.
[34] W. Huang et al., "Current-based open-circuit fault diagnosis for PMSM drives with model predictive control," *IEEE Trans. Power Electron.*, vol. 36, no. 9, pp. 10695–10704, Jun. 2021.
[35] X. Wang, Z. Wang, Z. Xu, M. Cheng, W. Wang, and Y. Hu, "Comprehensive diagnosis and tolerance strategies for electrical faults and sensor faults in dual three-phase PMSM drives," *IEEE Trans. Power Electron.*, vol. 34, no. 7, pp. 6669–6684, Jul. 2019.
[36] X. Wang, Z. Wang, Z. Xu, J. He, and W. Zhao, "Diagnosis and tolerance of common electrical faults in t-type three-level inverters fed dual three-phase PMSM drives," *IEEE Trans. Power Electron.*, vol. 35, no. 2, pp. 1753–1769, Feb. 2020.
[37] J. Hang, J. Zhang, M. Cheng, and S. Ding, "Detection and discrimination of open-winding fault in permanent magnet synchronous motor drive system," *IEEE Trans. Power Electron.*, vol. 31, no. 7, pp. 4697–4709, Jul. 2016.
[38] Y. Zhang, Y. Mao, X. Wang, Z. Wang, D. Xiao, and G. Fang, "Current prediction-based fast diagnosis of electrical faults in PMSM drives," *IEEE Trans. Transp. Electrific.*, vol. 8, no. 4, pp. 4622–4632, Dec. 2022.
[39] C. Choi, K. Lee, and W. Lee, "Observer-based phase-shift fault detection using adaptive threshold for rotor position sensor of permanent-magnet synchronous machine drives in electromechanical brake," *IEEE Trans. Ind. Electron.*, vol. 62, no. 3, pp. 1964–1974, Mar. 2015.
[40] H. Dan, W. Yue, W. Xiong, Y. Liu, M. Su, and Y. Sun, "Open-switch and current sensor fault diagnosis strategy for matrix converter-based PMSM drive system," *IEEE Trans. Transp. Electrific.*, vol. 8, no. 1, pp. 875–885, Mar. 2022.

Xinxiu Zhou (Member, IEEE) received the B.S. degree in motor drives and control and power electronic devices from Yanshan University, Hebei, China, in 2006, and the Ph.D. degree in the area of attitude control system technology of spacecraft and novel inertial instrument and equipment technology from Beihang University, Beijing, China, in 2013.

She is currently a Professor with the Research Institute for Frontier Science, Beihang University. Her research interests include motor control, power electron, spacecraft attitude control, and atomic gyro control.

Qingyao Hu received the B.S. degree in mechanical engineering from Beijing University of Technology, Beijing, China, in 2020. She is currently pursuing the M.S. degree in electronic information with the School of Instrumentation Science and Optoelectronics Engineering and Astronautics, Beihang University, Beijing, China.

Her research interests include fault diagnosis of permanent-magnet synchronous motor.

Peiling Cui (Member, IEEE) was born in Henan, China, in 1975. She received the Ph.D. degree in control theory and control engineering from Northwestern Polytechnical University, Xi'an, China, in 2004.

She is currently an Associate Professor in Instrumentation Science and Technology with the School of Instrumentation and Optoelectronic Engineering, Beihang University, Beijing, China. Her main research interests include active vibration control of magnetically suspended rotor.

Xueping Xu received the B.S. degree in mechanical engineering from Huazhong University of Science and Technology, Wuhan, China, in 2013, and the Ph.D. degree in mechanical engineering from Tsinghua University, Beijing, China, in 2018.

He is currently an Associate Professor with the School of Instrumentation and Optoelectronic Engineering, Beihang University, Beijing, China. His research interests include rotor dynamic analysis of electric motors.

Kun Mao received the B.S. degree from the Southwest University of Science and Technology, Mianyang, China, in 2009, and the M.S. and Ph.D. degrees in precision instrument and machinery from Beihang University, Beijing, China, in 2012 and 2018, respectively.

He is currently a Lecturer with the School of Instrumentation Science and Optoelectronics Engineering, Beihang University. He is also a Research Member with the Key Laboratory of Fundamental Science, National Defense, Novel Inertial Instrument and Navigation System Technology, Beihang University. His research interests include power electronics and high-speed permanent magnet motor control.